GEOPHYSICAL RESEARCH LETTERS, VOL. 25, NO. 6, PAGES 877-880, MARCH 15, 1998

Banded electron structure formation in the inner magnetosphere

M. W. Liemohn,[1] G. V. Khazanov,[2] and J. U. Kozyra[3]

Abstract. Banded electron structures in energy-time spectrograms have been observed in the inner magnetosphere concurrent with a sudden relaxation of geomagnetic activity. In this study, the formation of these banded structures is considered with a global, bounce-averaged model of electron transport, and it is concluded that this structure is a natural occurrence when plasma sheet electrons are captured on closed drift paths near the Earth followed by an extended period of quiet time for more than a day. These bands do not appear unless there is capture of plasma sheet electrons; convection along open drift paths making one pass around the Earth do not have time to develop this feature. The separation of high-energy bands from the injected population due to the preferential advection of the gradient-curvature drift creates spikes in the energy distribution above a keV, which overlap to form a series of bands in energy. The lowest band is the bulk of the injected population in the sub-keV energy range. Using the *Kp* history for an observed banded structure event, a cloud of plasma sheet electrons is captured and the formation of their distribution function is examined.

Introduction

In the recent study by *Burke et al.* [1995], the low-energy plasma analyzer (LEPA) instrument on the Combined Release and Radiation Effects Satellite (CRRES) detected several bands of magnetically trapped 0.1-30 keV electrons inside the plasmapause. They saw the high energy bands (E ≥ 1 keV) several orbits before seeing the low-energy band peaked below 1 keV. The formation of the high-energy bands are not discussed, and the only explanation for the low-energy band is that plasma sheet electrons were captured on corotating field lines by the time-dependent movement of the Alfvén boundary. These peaks in the energy spectra persist for several days, slowly spreading inward with a decrease in intensity and an increase in peak energy.

This study uses our bounce-averaged, time-dependent, global, kinetic model of electron transport to simulate the advection of plasma sheet electrons into the inner magnetosphere with the specific objective of determining the processes responsible for capturing the plasma sheet electrons and for creating these peaks in the electron energy distribution.

[1]Space Sciences Laboratory, NASA Marshall Space Flight Center, Huntsville, Alabama
[2]Physics Department, Geophysical Institute, University of Alaska Fairbanks
[3]Space Physics Research Laboratory, University of Michigan, Ann Arbor

Paper number 98GL00411.
0094-8534/98/98GL-00411$05.00

The Model

Our model of superthermal electron transport [*Khazanov et al.*, 1996] calculates the distribution on a global scale throughout the inner magnetosphere using a time-dependent kinetic approach. When the flight time along the magnetic field line, τ_b, is very short compared to the collisional timescales, which is the case for electrons above a few tens of eV, it is possible to average the particle fluxes along the field line over a magnetic mirror bounce period, yielding the bounce-averaged kinetic equation [*Jordanova et al.*, 1996; *Khazanov et al.*, 1996],

$$\frac{\partial\langle f\rangle}{\partial t}+\left\langle \vec{V}_D\right\rangle\frac{\partial\langle f\rangle}{\partial \vec{R}_\perp}+\left\langle\frac{dE}{dt}\right\rangle\frac{\partial\langle f\rangle}{\partial E}+\left\langle\frac{d\mu_0}{dt}\right\rangle\frac{\partial\langle f\rangle}{\partial\mu_0} = \left\langle\frac{\delta f}{\delta t}\right\rangle_{CC}-\frac{\langle f\rangle}{0.5\tau_b} \quad (1)$$

where f is the particle distribution function, $\vec{V}_D$ is the perpendicular drift velocity, $\vec{R}_\perp$ includes the spatial directions perpendicular to the magnetic field, E is energy, μ_0 is the cosine of the particle pitch angle at the geomagnetic equator, and $\langle\xi\rangle$ denotes averaging ξ over a bounce period along the field line. The collisional process on the right hand side is Coulomb interactions with the thermal plasma, and atmospheric precipitation is treated as a differential loss each half bounce period.

In order to model the injection of plasma sheet electrons into the inner magnetosphere, it is necessary to determine where along the outer boundary of the simulation domain the injection is occurring. This can be done by solving the system of equations consisting of the four bounce-averaged drift velocities $\left(\langle dR/dt\rangle, \langle d\varphi/dt\rangle, \langle dE/dt\rangle, \langle d\mu_0/dt\rangle\right)$ for the particle drift paths. Under steady geomagnetic activity, this yields trajectories that are either open (enter from the tail and exit through the dayside boundary) or closed (returning to their point of origin). The separatrix between these open and closed trajectories is known as the Alfvén boundary, and his early work in this area is summarized in *Alfvén and Fälthammar* [1963]. The location of this boundary is a function of particle energy and pitch angle as well as geomagnetic activity. For electrons, the gradient-curvature drift is in the same direction as the corotation drift, and thus the Alfvén boundary for higher-energy electrons will be further out than that for low-energy particles. While a decrease in corotation period is evident for all energies, the expansion of the Alfvén boundary becomes noticeable for energies greater than a few keV, and becomes the dominant azimuthal drift term. While the energy dependence is important, it should be noted that the pitch angle dependence is very modest and only becomes a factor for high-energy electrons.

This boundary, however, is highly dependent on geomagnetic activity. The Alfvén boundaries for several energies and *Kp* values are shown in Figure 1. The difference between the boundaries at *Kp*=1 and *Kp*=5 is quite evident, with the low

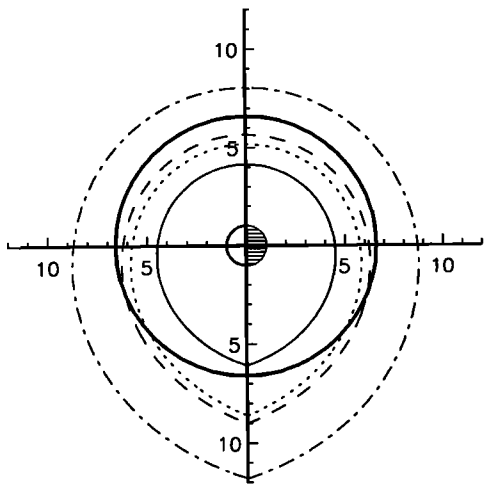

Figure 1. View in the equatorial plane of electron Alfvén boundaries relative to the simulation domain (bold solid line) for given activity and energy. The Kp=5 boundary for E=50 keV (solid line) is shown, along with Kp=1 boundaries for E=0.5 keV (dotted line), E=5.0 keV (dashed line), and E=50 keV (dash-dot line). All energies are for when the particle is at dusk, with a pitch angle of 80°.

activity boundary for a 50 keV electron at φ=1800 h (dash-dot line) completely outside of the simulation outer boundary (bold solid line at geosynchronous orbit) and the high activity boundary for the same energy (solid line) is completely within the simulation outer boundary. The other two Alfvén boundaries shown are for E=0.5 keV (dotted line) and E=5.0 keV (dashed line) at φ=1800 h. Therefore the particles entering through the outer boundary of the simulation domain will not always be the plasma sheet distribution. The location in φ of the Alfvén boundary at this outer radial distance, $\varphi_B(E, \mu_0, Kp)$, must be accurately determined, with injected plasma sheet particles entering along the open trajectories (dawnward of φ_B) and some other boundary condition for the closed trajectories (duskward of φ_B), here chosen as a slow cororation from the dayside. For this study, φ_B was calculated and tabulated for use during the simulations, so that the appropriate boundary condition is taken for each energy and pitch angle at each azimuthal angle for each time step.

Finally, the model can assume any initial or boundary condition. In order to focus on the injection of plasma sheet electrons from the nightside during this capture event in early 1991 seen by the CRRES satellite [*Burke et al.*, 1995], we begin these simulations with only thermal plasma inside the simulation domain (calculated from the *Rasmussen et al.* [1993] plasmasphere model), and with a boundary condition on the nightside (dawnward of φ_B) consistent with a quiet time plasma sheet. A survey of the near-Earth plasma sheet during quiet geomagnetic periods [*Christon et al.*, 1989] concluded that the plasma sheet is best modeled with an isotropic kappa distribution, where the energy dependence is roughly Maxwellian below the characteristic energy E_0 and becomes a power law at higher energies with $f \propto E^{-\kappa-1}$. They found that the mean values for electrons are κ=6 and E_0=0.2 keV, and these values will be used in the present study. The density of the injected electrons during this relatively quiet time is taken to be 0.1 cm^{-3} [Cf., *Huang and Frank*, 1986; *Baumjohann et al.*, 1989; *Christon et al.*, 1989; *Birn et al.*, 1997]. While it would be more accurate to use measured fluxes at geosynchronous orbit for the injected distribution function, this is beyond the scope of the present study, and these values for the kappa function are taken as constant throughout the simulations to be discussed.

Results

The Kp history for late January 1991 is shown in Figure 2. The simulations are started on January 25 to allow for the build-up of the injected population in the inner magnetosphere before the days of interest, January 28-30. It is thought that the drop from Kp=3 to Kp=1 between January 28 and 29 is responsible for capturing a cloud of low-energy electrons along closed drift paths. A higher-energy band already existed at these radial distances, presumably captured by earlier decreases in activity. It is the goal of this study to quantitatively determine the reason for the formation of these bands in the energy distribution function.

The observations discussed by *Burke et al.* [1995] are shown as energy-time spectrograms for ~90° pitch angle as the satellite swept through the nightside magnetosphere (out near geosynchronous orbit). Because apogee at this time period was near local midnight, time is somewhat analogous to radial distance. In order to qualitatively compare with these measurements, results from the simulation are shown in Plate 1 as energy vs. radial distance spectrograms at 90° pitch angle at local midnight for 10 times during the simulation. The first spectrogram is one day into the simulation, the second 2 days, the fourth 3 days, and the twelfth (last) one is after six days of simulation. Several bands in the energy spectrum are clearly visible, and it appears that a cloud of sub-keV electrons is trapped early and remains throughout the simulation. The magnitude of this population decreases with time, and it rotates around the globe with slightly less than a 24 hour period due to the gradient-curvature drift adding to the corotation drift.

The banded structure of the captured plasma sheet electrons is clearly seen in Figure 3, showing energy flux spectra at 90° pitch angle and local midnight at three radial distances for successive passes of the peak in the captured cloud. The slow decrease in the intensity of this band is clearly evident, while the high-energy bands do not suffer from the same degradation. This degradation is due to the slow Coulomb scattering of particles into the loss cone, and it is seen that the intensity does not change appreciably until several days have passed. It is also seen that the low-energy peak decreases in energy at smaller radial distances. This is also due to Coulomb colli-

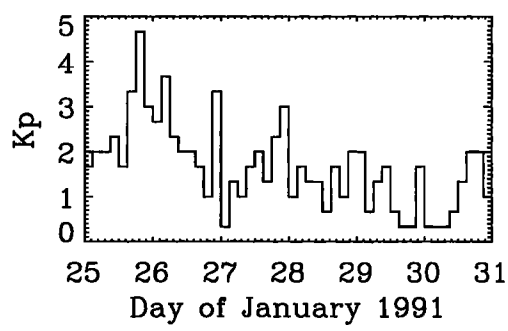

Figure 2. Kp history during the CRRES observations of the banded electron structures.

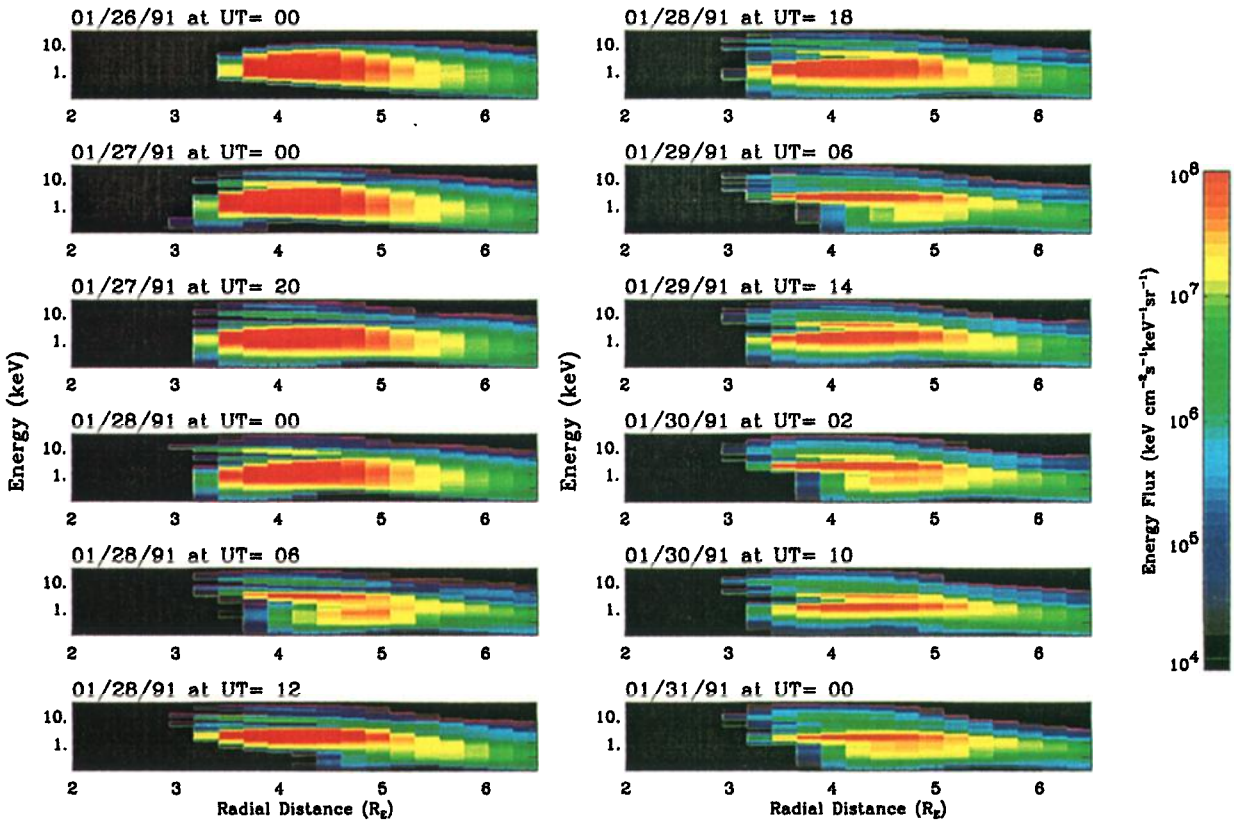

Plate 1. Energy vs. radial distance spectrograms for 90° pitch angle at local midnight at various times throughout the simulation, qualitatively analogous to the spectrograms in *Burke et al.* [1995]. Notice the appearance and disappearance of the low-energy band below 1 keV.

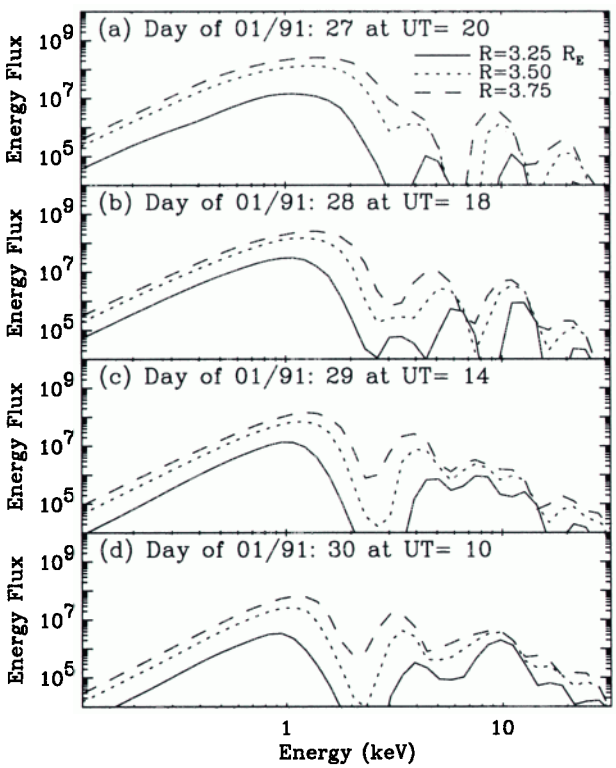

Figure 3. Energy spectra of the peak in the cloud at 90° pitch angle for successive passes of local midnight at radial distances of 3.25 R_E (solid line), 3.50 R_E (dotted line), and 3.75 R_E (dashed line).

sions, consistent with the increase in thermal plasma at the smaller radial distances. The magnitude of the high-energy peaks fluctuates greatly in these plots because these peaks rotate with a shorter period due to the super-corotative effect of magnetic drifts on electrons.

It was mentioned in *Burke et al.* [1995] that these banded structures were strongly peaked at 90° pitch angle. Figure 4 shows the energy spectra for three pitch angles at R=3 R_E both inside and outside of the low-energy cloud of captured plasma sheet electrons. An order of magnitude decrease in energy flux is evident between the trapped particles and those near the loss cone. The pitch angles inside the loss cone, with the atmospheric loss term shown in (1), are many orders of magnitude less intense than these pitch angles. It is interesting to note that the high energy bands are quite smeared as the pitch angle dependence of the azimuthal acts to spatially spread these peaks.

Discussion

It is clear that the model reproduces the banded energy structure in the distribution of captured plasma sheet electrons. Let us now discuss the processes involved in its formation.

Similar calculations to those presented above, except with constant *Kp* histories (high or low, not plotted), do not result in a captured population, and the banded structures do not persist past a day of simulation time. Outside the (energy dependent) Alfvén boundary, the particles drift past the Earth and out the dayside boundary, and the region within the boundary remains essentially empty. A slight banded structure appears

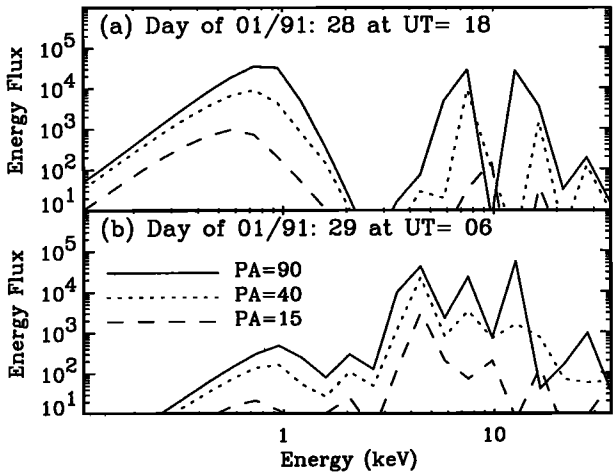

Figure 4. Energy spectra inside (upper panel) and outside (lower panel) of the low-energy cloud at 3 R_E and local midnight for pitch angles of 90° (solid line), 40° (dotted line), and 15° (dashed line).

during the early stages of the simulation before the bulk of the kappa distribution has filled in the open trajectories. During these times, the high-energy electrons outpace the low-energy particles resulting in a spike in the energy spectrum that stretches out around the dawn side of the inner magnetosphere. Once the low-energy electrons have propagated around, no bands remain and a steady-state solution has been reached.

Also, a simulation without the ramp and sudden drop in *Kp* on January 28 (not plotted) still exhibits a banded structure but the features are less intense. Because there are low-energy particles captured along closed drift paths from the earlier drops in *Kp*, the intensity is less but the cloud still exists. One factor contributing to the observations of this phenomenon by CRRES is that the three Kp spikes are exactly 24 hours apart, and so these injections build up a low-energy cloud in the same longitude band. The high-energy electrons, which have a less than 24 hour closed drift path period due to magnetic drift, are not built up in such a constructive manner, contributing to their seemingly constant presence in Plate 1.

From further simulations, it was determined that the azimuthal drift term is the important factor in forming this feature. This drift can be written as

$$\left\langle \frac{d\varphi}{dt} \right\rangle = \frac{C}{M_E} + \frac{AR^3 \sin\varphi}{M_E} - \frac{3ER}{qM_E}\left[1 - \frac{I(\mu_0)}{6h(\mu_0)}\right] \qquad (2)$$

where A is a function of geomagnetic activity , C is a constant characterizing the corotation electric field, M_E is the magnetic dipole of the Earth, q is the charge of the particle including sign, and $I(\mu_0)$ and $h(\mu_0)$ are slowly-varying functions of equatorial pitch angle resulting from the bounce-averaging process [*Ejiri*, 1978]. On the right-hand side, the first term is due to corotation, the second is due to convection from the tail, and the third is due to the gradient and curvature of the magnetic field. It was determined that this last term in (2) is the primary cause of the banded structure. The extra eastward drift from this term causes high-energy electrons to circle the globe much faster than those of lower energy, and this preferential drift eventually causes the series of spikes in the energy distribution function seen in the figures. Without this term, the distribution function remains a kappa distribution throughout the simulation.

We have shown that this multiply-peaked distribution function is a natural occurrence in the inner magnetosphere due to the energy-dependent drift of the electrons, and that this should occur any time plasma sheet electrons are captured on closed drift paths followed by an extended quiet period of more than a day. This was done by simulating the time period of the January 1991 observations in the *Burke et al.* [1995] study and investigating the physical processes influencing the motion of the electrons. Further investigations will examine the energy degradation of this captured cloud of electrons and the relative importance of the various decay processes.

Acknowledgments. This work was supported by the National Science Foundation under contracts ATM-9710326 and ATM-9896049, and MWL worked under a National Research Council Postdoctoral Associateship at NASA MSFC.

References

Alfvén, H., and C.-G. Fälthammar, *Cosmical Electrodynamics*, Oxford University Press, London, 1963.

Baumjohann, W., G. Paschmann, and C. A. Cattell, Average plasma properties in the central plasma sheet, *J. Geophys. Res.*, *94*, 6597, 1989.

Birn, J., M. F. Thomsen, J. E. Borovsky, G. D. Reeves, D. J. McComas, and R. D. Belian, Characteristic plasma properties during dispersionless substorm injections at geosynchronous orbit, *J. Geophys. Res.*, *102*, 2309, 1997.

Burke, W. J., A. G. Rubin, D. A. Hardy, and E. G. Holeman, Banded electron structures in the plasmasphere, *J. Geophys. Res.*, *100*, 7759, 1995.

Christon, S. P., D. J. Williams, D. G. Mitchell, L. A. Frank, and C. Y. Huang, Spectral characteristics of plasma sheet ion and electron populations during undisturbed geomagnetic conditions, *J. Geophys. Res.*, *94*, 13,409, 1989.

Ejiri, M., Trajectory traces of charged particles in the magnetosphere, *J. Geophys. Res.*, *83*, 4798, 1978.

Harel, M., R. A. Wolf, P. H. Reiff, R. W. Spiro, W. J. Burke, F. J. Rich, and M. Smiddy, Quantitative simulation of a magnetospheric substorm 1. Model logic and overview, *J. Geophys. Res.*, *86*, 2217, 1981.

Huang, C. Y., and L. A. Frank, A statistical study of the central plasma sheet: Implications for substorm models, *Geophys. Res. Lett.*, *13*, 652, 1986.

Jordanova, V. K., L. M. Kistler, J. U. Kozyra, G. V. Khazanov, and A. F. Nagy, Collisional losses of ring current ions, *J. Geophys. Res.*, *101*, 111, 1996.

Khazanov, G. V., T. E. Moore, M. W. Liemohn, V. K. Jordanova, and M.-C. Fok, Global, collisional model of high-energy photoelectrons, *Geophys. Res. Lett.*, *23*, 331, 1996.

Rasmussen, C. E., S. M. Guiter, and S. G. Thomas, Two-dimensional model of the plasmasphere: refilling time constants, *Planet. Space Sci.*, *41*, 35, 1993.

M. W. Liemohn, Space Sciences Laboratory, NASA Marshall Space Flight Center, Mail Code ES-83, Huntsville, AL 35812. (email: mike.liemohn@msfc.nasa.gov)

G. V. Khazanov, Geophysical Institute, University of Alaska Fairbanks, P.O. Box 757320, Fairbanks, Alaska 99775-7320. (email: khazanov@gi.alaska.edu)

J. U. Kozyra, 2455 Hayward St.., University of Michigan, Ann Arbor, MI 48109-2143. (email: jukozyra@engin.umich.edu)

(Received October 14, 1997; accepted January 16, 1998.)